Proton-Induced Radiation Damage in Fast Crystal Scintillators

Fan Yang, *Member, IEEE*, Liyuan Zhang, *Member, IEEE*, Ren-Yuan Zhu, *Senior Member, IEEE*, Jon Kapustinsky, *Senior Member, IEEE*, Ron Nelson, and Zhehui Wang, *Member, IEEE*

***Abstract*— This paper reports proton-induced radiation damage in fast crystal scintillators. Large size LYSO and CeF_3 crystals of 20 and 15 cm long were irradiated by 800 MeV protons at Los Alamos up to 3.3×10^{14} p/cm^2 with degradation and recovery of their longitudinal transmittance measured *in situ*. LYSO plates of $14 \times 14 \times 1.5$ mm^3 were irradiated by 67 MeV protons at UC Davis up to 9.5×10^{13} p/cm^2, and by 24 GeV protons at CERN up to 6.9×10^{15} p/cm^2. The results show an excellent radiation hardness of LYSO crystals against charged hadrons.**

***Index Terms*— Crystals, LYSO, protons, radiation damage, scintillators.**

I. Introduction

BECAUSE of their superb energy resolution and detection efficiency, crystal scintillators are widely used in HEP experiments. The CMS lead tungstate ($PbWO_4$ or PWO) crystal calorimeter, for example, has played an important role in the discovery of the Higgs boson [1]. One crucial issue, however, is their radiation damage in a severe radiation environment, which requires precision monitoring to correct variations of crystal's transparency [2]. During the two years of the 1st run, for example, up to 70% loss of light output in CMS PWO crystals at large rapidity was observed *in situ* at the LHC when the experiment was running at a half of its designed energy with 5×10^{33} cm^{-2}s^{-1} luminosity [3]. The HL-LHC designed at 5×10^{34} cm^{-2}s^{-1} luminosity and up to 3,000 fb^{-1} integrated luminosity presents an extreme severe radiation environment, where up to 3×10^{14} charged hadrons/cm^2 (Fig.1) and 5×10^{15} neutral hadrons/cm^2 (Fig.2) are expected in addition to an ionization dose of up to 130 Mrad [4]. Cerium doped lutetium yttrium oxyorthosilicate ($Lu_{2(1-x)}Y_{2x}SiO_5$:Ce or LYSO) [5] and cerium fluoride [6] crystals were proposed to construct sampling Shashlik calorimeters for the CMS forward calorimeter upgrade for the HL-LHC. LYSO crystals were also proposed by the SuperB, Mu2e and COMET experiments to construct total absorption crystal calorimeters [7]–[9]. A crucial issue for these crystal based detector concepts is the crystal's survivability in the expected radiation environment.

Manuscript received March 25, 2016; revised November 23, 2016; accepted November 25, 2016. Date of publication November 29, 2016; date of current version February 28, 2017. This work was supported in part by the U.S. Department of Energy Grants DE-SC0011925 and DE-AC52-06NA25396.

F. Yang, L. Zhang, and R.-Y. Zhu are with the California Institute of Technology, Pasadena, CA 91125 USA (e-mail: zhu@hep.caltech.edu).

J. Kapustinsky, R. Nelson, and Z. Wang are with the Los Alamos National Laboratory, Los Alamos, NM 87545 USA.

Color versions of one or more of the figures in this paper are available online at http://ieeexplore.ieee.org.

Digital Object Identifier 10.1109/TNS.2016.2633427

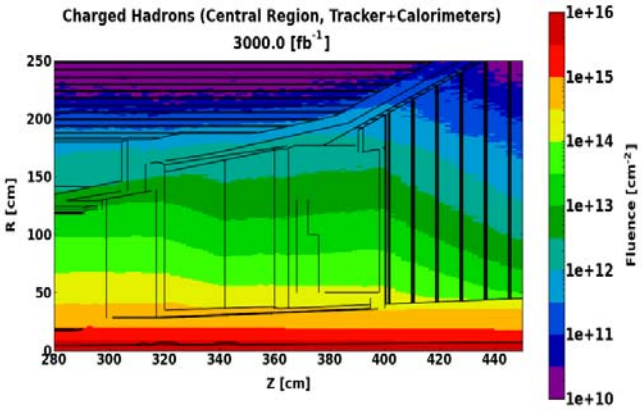

Fig. 1. The charged hadron fluence expected by the CMS endcap calorimeter for 3,000 fb^{-1} at the HL-LHC is shown in the R-Z plane [4].

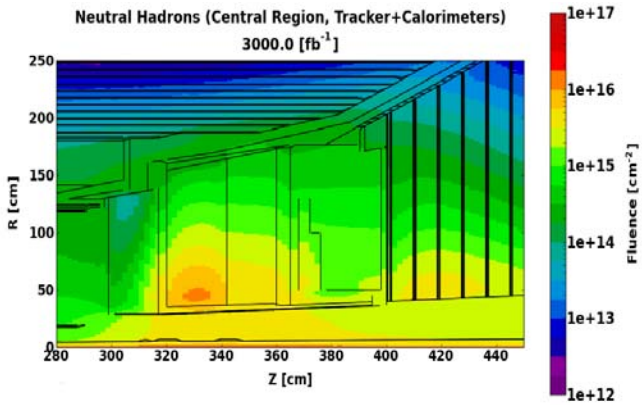

Fig. 2. The neutral hadron fluence expected by the CMS endcap calorimeter for 3,000 fb^{-1} at the HL-LHC is shown in the R-Z plane [4].

Proton-induced radiation damage was investigated for LYSO, CeF_3 and PWO [10]–[17]. Because of the radioactivity induced by protons in the crystals, all measurements were carried out several tens of days after irradiation. In this paper, we report proton-induced radiation damage in large size LYSO and CeF_3 crystals measured *in situ* before and immediately after radiation in the 800 MeV proton beam at LANL. In addition, results of thin LYSO plates irradiated by 67 MeV protons at UC Davis and 24 GeV protons at CERN are also reported. Fig. 3 shows the energy spectra of neutrons and charged hadrons expected by the CMS endcap electromagnetic calorimeter [18] at the LHC. While the energy of neutrons is peaked at a few MeV, it is several hundred MeV for charged

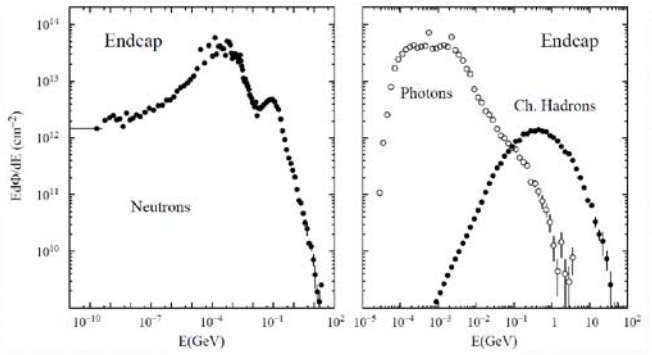

Fig. 3. The energy spectra of radiation background from neutrons, photons and charged hadrons expected by the CMS endcap calorimeter [18].

TABLE I
SAMPLES LOADED ON THE LINEAR STAGE AND THE PROTON FLUENCE

Sample	Dimension (cm^3)	Fluence (p/cm^2)
LYSO/W Shashlik Cell	$1.4 \times 1.4 \times 0.15$	-
Four Quartz Capillaries	Φ 0.1 × 6	2.7×10^{14}
OET-LFS	$2.5 \times 2.5 \times 18$	-
SG-LYSO	$2.5 \times 2.5 \times 20$	3.3×10^{14}
SIC-BGO	$2.5 \times 2.5 \times 20$	-
SIC-CeF_3	$2.2^2 \times 2.6^2 \times 15$	1.4×10^{14}

hadrons. The 800 MeV proton beam at LANL thus is ideal for this investigation.

II. SAMPLES AND EXPERIMENT

Table I lists the six samples prepared to be irradiated by the 800 MeV proton beam at the Weapons Neutron Research (WNR) facility of Los Alamos Neutron Science Center (LANSCE). Also listed in the table is the proton fluence calculated according to the beam current data provided by LANSCE. The overall uncertainty of the fluences is about 10%.

All six samples were loaded on a linear translation stage with a travel distance of 1 m, as shown in Fig. 4. The stage moved each individual sample into the proton beam via remote control. The 800 MeV proton beam had a Gaussian shape with a FWHM of about 2.5 cm and was aligned at the center of each sample in turn. Because of the large distance between the samples multiple scattering effects to the neighboring crystal was negligible.

Fig. 5 shows an optical fiber and a lock-in amplifier based spectrophotometer used to measure longitudinal transmittance *in situ* before and after irradiation for four long crystals. A part of the chopped light from a 150 W Xe lamp through a monochromator was monitored by a reference photodiode (Thorlabs DET10A). The main part of the light was injected into the crystal sample via ϕ0.365 mm quartz fibers and through two collimators at the front and back of the crystal, and was measured by a signal photodiode (Oriel 70336). The lock-in amplifier (Oriel Merlin) measured the ratio between the signal and reference photodetectors. The precision and stability of this ratio is better than 1%, and is free from both the radiation induced phosphorescence background in the sample

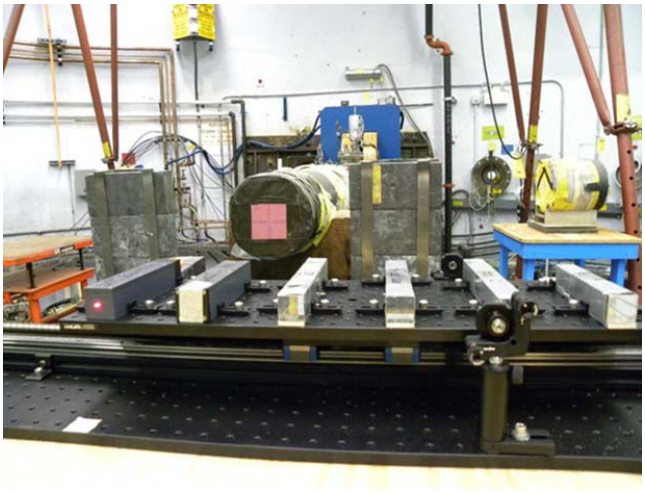

Fig. 4. A photo showing six samples loaded in a linear translation stage following the order listed in Tale I from left to right.

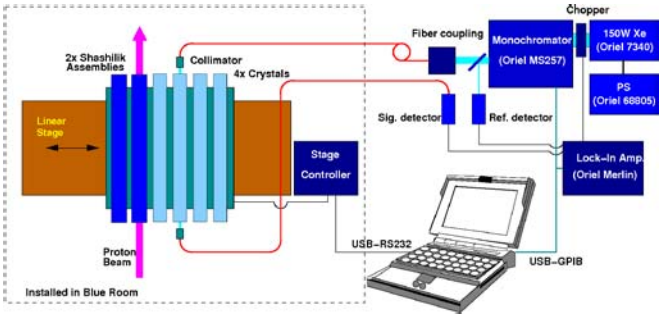

Fig. 5. A schematic showing the setup used to measure crystal's longitudinal transmittance *in situ* at Los Alamos.

TABLE II
PROTON FLUENCE ON LYSO PLATES

Sample ID	Dimension (mm^3)	Proton Energy	Proton Fluence (p/cm^2)
SIC603	$14 \times 14 \times 1.5$	67 MeV	1.2×10^{12}
SIC604	$14 \times 14 \times 1.5$	67 MeV	1.2×10^{12}
SIC605	$14 \times 14 \times 1.5$	67 MeV	1.2×10^{13}
SIC606	$14 \times 14 \times 1.5$	67 MeV	2.2×10^{13}
SIC607	$14 \times 14 \times 1.5$	67 MeV	9.5×10^{13}
SIC583	$14 \times 14 \times 1.5$	24 GeV	7.4×10^{13}
SIC594	$14 \times 14 \times 1.5$	24 GeV	2.3×10^{15}
SIC609	$14 \times 14 \times 1.5$	24 GeV	2.3×10^{15}
SIC001	$14 \times 14 \times 1.5$	24 GeV	6.9×10^{15}

and the fluctuations of the light intensity. Because of a power outage during the experiment only the quartz capillaries as well as the LYSO and CeF_3 crystals were irradiated to 2.7, 3.3 and 1.4×10^{14} p/cm^2 respectively, as shown in Table I.

To avoid the hadronic shower leakage effect in long crystals, nine LYSO plates of $14 \times 14 \times 1.5$ mm^3 were also irradiated at UC Davis by 67 MeV protons with a FWHM of 25 mm up to 9.5×10^{13} p/cm^2, and at CERN by 24 GeV protons with a FWHM of 12 mm up to 6.9×10^{15} p/cm^2. Table II lists the proton fluence that went through these samples. The uncertainty of the Davis fluence is about 10%., At CERN it was 7% as provided by the CERN IRRAD proton facility which was calibrated by activation of Al foils.

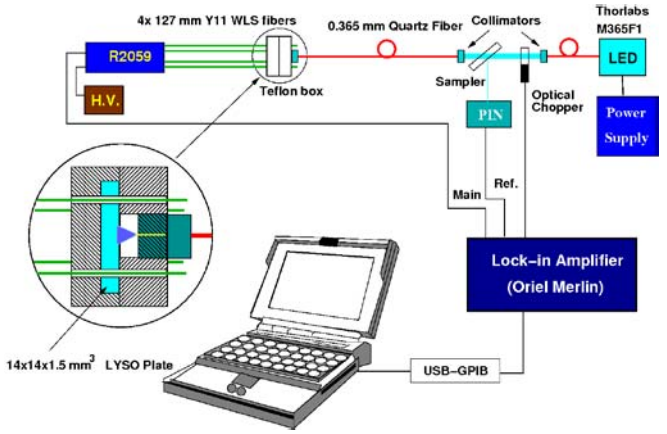

Fig. 6. A schematic showing the setup used to measure the light output of LYSO plates with strong phosphorescence after proton irradiation.

All samples were measured at Caltech before and about 80 days after irradiation. Transmittance was measured by a PerkinElmer Lambda 950 spectrophotometer with 0.15% precision. The precision for the corresponding radiation induced absorption coefficient (RIAC, see below for the definition) is about 3.5 m^{-1} for 1.5 mm thick LYSO plates, and is much less for long crystals.

Light output of LYSO plates before and after irradiation with a proton fluence of less than 10^{14}p/cm^2 with an air gap coupled to a Hamamatsu R2059 PMT was measured by using 0.511 MeV γ-rays from a ^{22}Na source. The systematic uncertainty of this measurement is about 1%. Because of the strong residual phosphorescence background, the light output of the LYSO plates after more than 10^{14} p/cm^2 was also measured as the intensity of photoluminescence. Fig. 6 shows the setup used for this measurement, where the LYSO sample surrounded by a Teflon box was excited by a 365 nm LED and read out by four Y-11 wavelength shifting fibers (WLS) fibers. A lock-in amplifier was also used in this setup to mitigate the residual phosphorescence in the samples. The corresponding systematic uncertainty of this measurement is about 1.5% estimated by repeated measurements for one sample.

III. Results of the Long CeF_3 Sample

Fig. 7 shows the longitudinal transmittance spectra of the CeF_3 crystal sample measured before and after a proton fluence of 1.4×10^{14} p/cm^2, and during the recovery. Also listed in the figure are the numerical values of longitudinal transmittance at 340 nm which is around the emission peak of γ-ray stimulated scintillation in CeF_3 [14].

While the spectra before and 84 and 392 days after the proton irradiation were measured by the PerkinElmer LAMBDA 950 spectrophotometer at Caltech, the others were measured *in situ* by using the on-line monitoring setup shown in Fig. 5.

Fig. 8 shows the radiation induced absorption coefficient (RIAC) spectra for the CeF_3 sample. The RIAC and EWRIAC represent radiation damage in crystal's transparency, and are defined as [17], [19]:

$$RIAC = \frac{1}{l} ln \frac{T_0(\lambda)}{T(\lambda)} \tag{1}$$

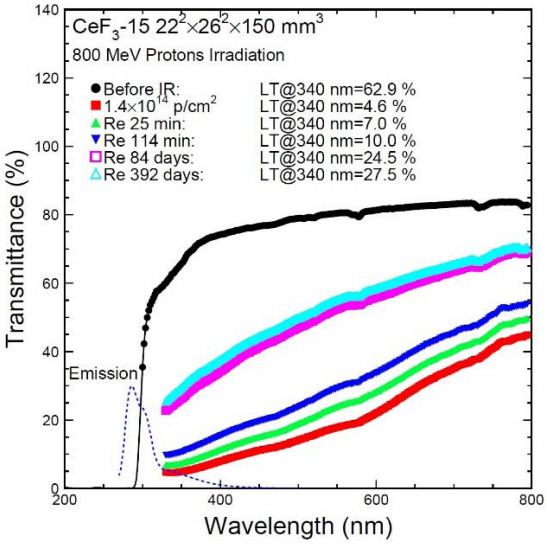

Fig. 7. The longitudinal transmittance spectra measured before and after proton irradiation for the sample SIC-CeF_3.

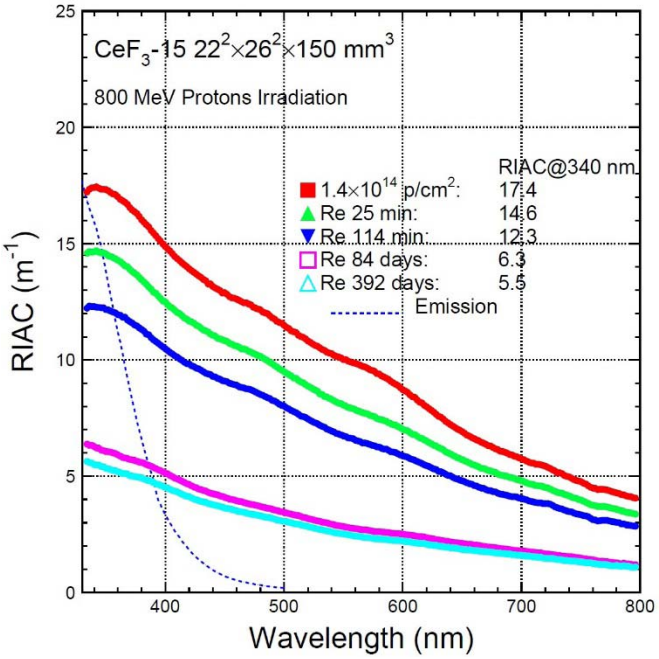

Fig. 8. The RIAC spectra measured after proton irradiation are shown for the sample SIC-CeF_3.

$$EWRIAC = \frac{\int RIAC(\lambda)\, Em(\lambda)\, d\lambda}{\int Em(\lambda)\, d\lambda} \tag{2}$$

where T_0 and T are the transmittance along crystal length l measured before and after irradiation; $Em(\lambda)$ is the emission spectrum. The numerical values of the RIAC at 340 nm are also listed in this figure. It was 17.4 m^{-1} after a proton fluence of 1.4×10^{14} p/cm^2, indicating severe radiation damage caused by protons in this CeF_3 sample.

Fig. 9 shows the RIAC values at 340 nm as a function of the recovery time for SIC-CeF_3 after a proton fluence of 1.4×10^{14} p/cm^2. The top and bottom plots show recovery in short and long time scale respectively with recovery time

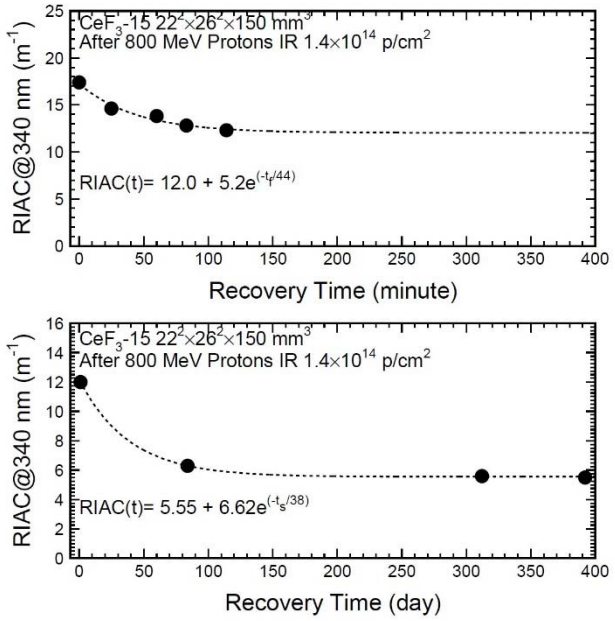

Fig. 9. The recovery of proton-induced radiation damage for SIC-CeF_3.

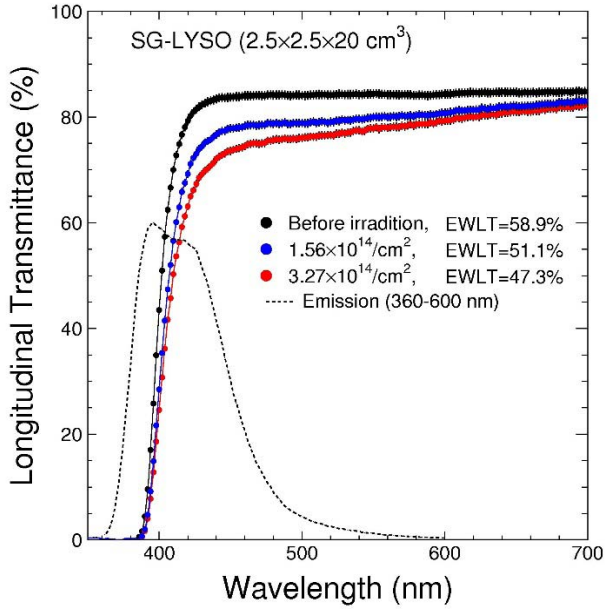

Fig. 10. The longitudinal transmittance spectra measured after each irradiation step are shown for the sample SG-LYSO.

constants of 44 minutes and 38 days extracted by exponential fits. While the short recovery may be partially caused by a temperature relaxation because of the high temperature of the sample after irradiation, the long recovery time constant shows a clear recovery at room temperature (293 K) in the CeF_3 crystal after proton irradiation. The RIAC value at 340 nm is 5.6 m^{-1} after 392 days, indicating additional deep absorption centers in the crystal with an even slower recovery time constant.

IV. Results of the Long LYSO Sample

The long LYSO sample (SG-LYSO) was irradiated in two steps. Fig. 10 shows the longitudinal transmittance spectra

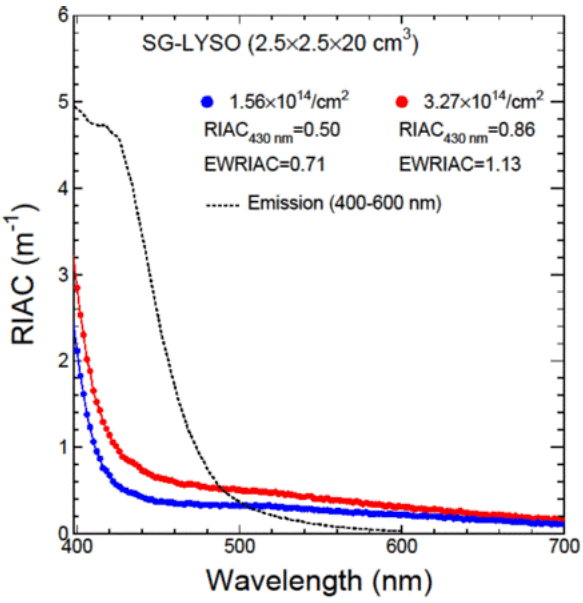

Fig. 11. The RIAC spectra measured after each irradiation step are shown for the sample SG-LYSO.

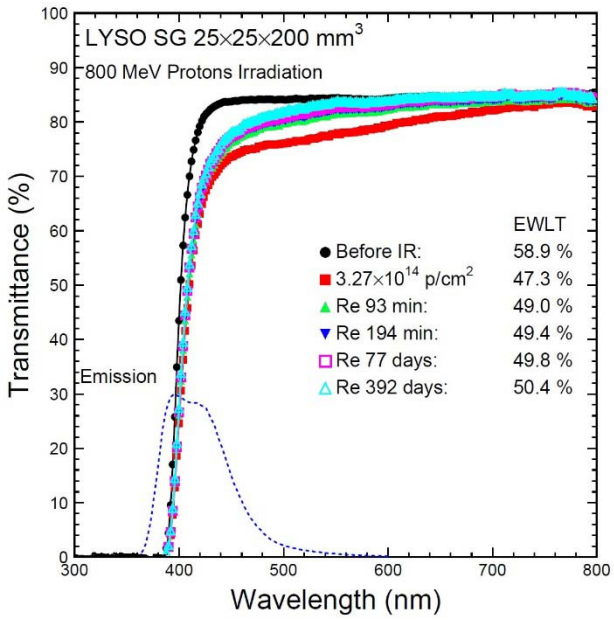

Fig. 12. The longitudinal transmittance spectra measured before and after irradiation are shown for the sample SG-LYSO.

measured before and after irradiation of 1.6×10^{14} and 3.3×10^{14}p/cm^2. Also listed in the figure are the numerical values of the emission weighted longitudinal transmittance (EWLT) which is defined as [19]:

$$EWLT = \frac{\int LT(\lambda)\, Em(\lambda)\, d\lambda}{\int Em(\lambda)\, d\lambda} \tag{3}$$

The EWLT value provides a numerical representation of the longitudinal transmittance data across the emission spectrum. It is a direct measure of transparency for crystal's scintillation light. The EWLT loss is at a level of 20% after 3.3×10^{14} p/cm^2.

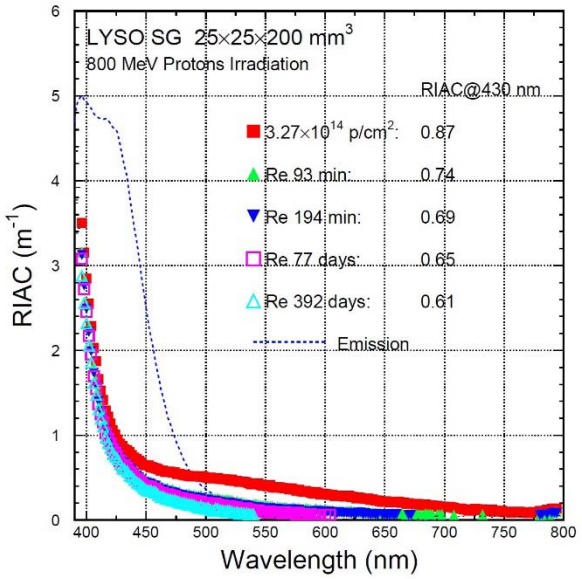

Fig. 13. The RIAC spectra measured after irradiation are shown for the SG LYSO sample.

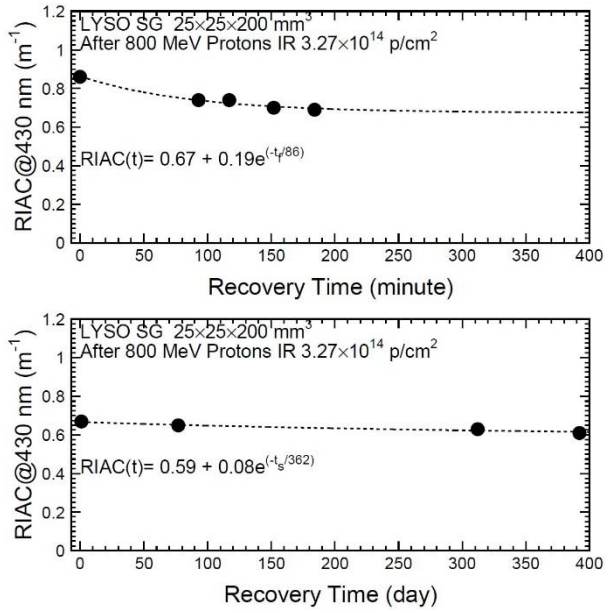

Fig. 14. The recovery of proton-induced radiation damage for SG-LYSO

The corresponding RIAC spectra are shown in Fig. 11. Also listed in the figure are the values of both the EWRIAC and the RIAC at 430 nm. After a proton fluence of 3.3×10^{14} p/cm^2 this LYSO sample has a EWRIAC value of 1.1 m^{-1}, indicating its excellent radiation hardness against protons.

Fig. 12 shows the longitudinal transmittance spectra together with the EWLT values for the LYSO sample before irradiation and during recovery after 3.3×10^{14} p/cm^2. While the spectra before irradiation and 77 and 392 days after irradiation were measured by the PerkinElmer LAMBDA 950 spectrophotometer at Caltech, the others were measured *in situ* by using the on-line monitoring setup shown in Fig. 5. It is interesting to note that the recovery is very small after the 1st hour even with thermal relaxation.

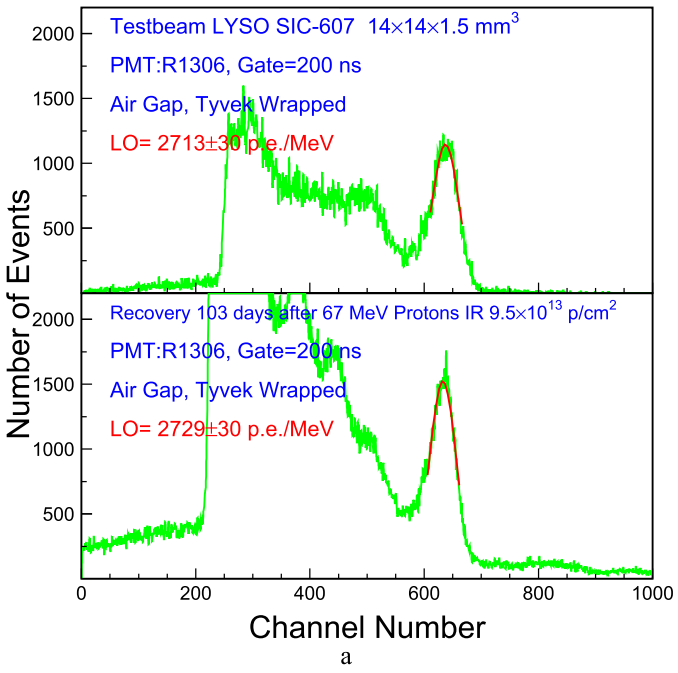

a

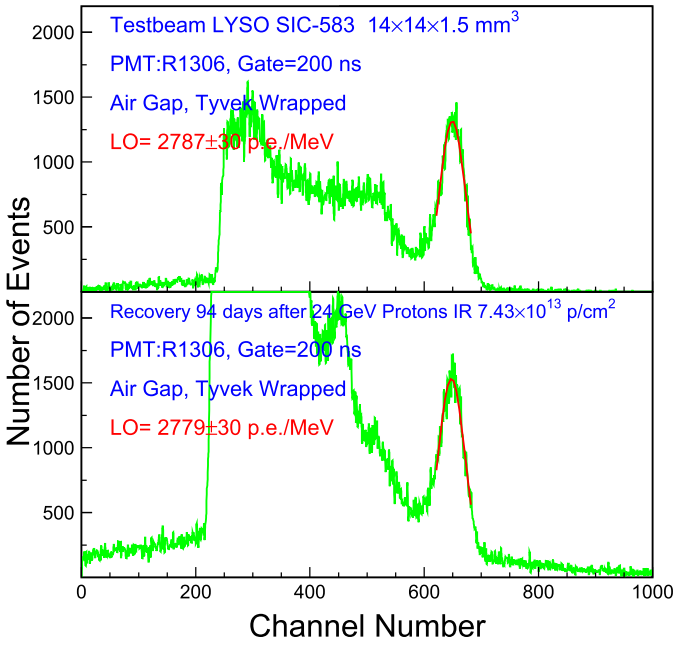

b

Fig. 15. Pulse height spectra of 0.511 MeV γ-rays from a ^{22}Na source are shown for LYSO plates after proton irradiation of (a) 9.5×10^{13}p/cm^2 by 67 MeV protons and (b) 7.4×10^{13}p/cm^2 by 24 GeV protons.

Fig. 13 shows the RIAC spectra for the long LYSO sample after 3.3×10^{14} p/cm^2 during recovery. The numerical values of RIAC at 430 nm are also shown in the figure.

Fig. 14 shows the RIAC value at 430 nm as a function of recovery time for the long LYSO sample after 3.3×10^{14} p/cm^2. While the upper figure shows the recovery in a few hundred minutes measured *in situ*, the bottom figure shows a few hundred days measured at Caltech under room temperature. The recovery time constants determined

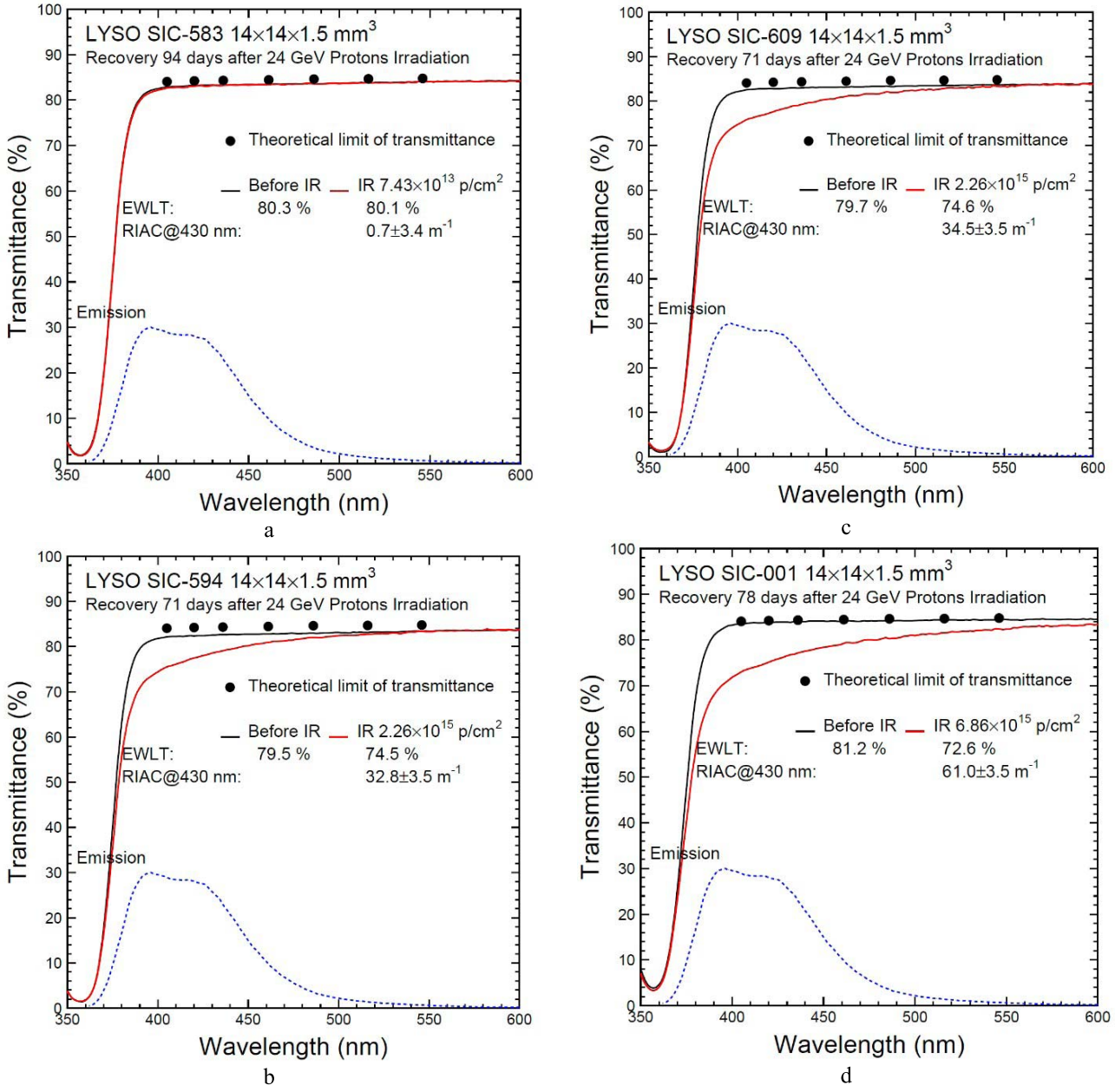

Fig. 16. Transmittance of LYSO plates of $14 \times 14 \times 1.5$ mm^3 after 24 GeV proton irradiation. a) Sample 583 irradiated to 7.4×10^{13}p/cm^2; b) Sample 594 irradiated to 2.3×10^{15}p/cm^2; c) Sample 609 irradiated to 2.3×10^{15}p/cm^2; and d) Sample 001 irradiated to 6.9×10^{15}p/cm^2

by exponential fits are 86 minutes and 362 days respectively. As discussed, the fast recovery is suspected to be caused by a thermal relaxation since the sample was several tens of degrees higher than the room temperature after the proton fluence of 3.3×10^{14} p/cm^2. The small recovery amplitude of 0.08 m^{-1} under room temperature indicates that the recovery of proton-induced radiation damage in LYSO crystal is very small.

V. Results of the LYSO Plate Samples

LYSO plates of $14 \times 14 \times 1.5$ mm^{3}are used to construct a prototype LYSO/W Shashlik calorimeter matrix [5]. Several plates were irradiated at UC Davis (67 MeV) and CERN (24 GeV) by protons. Fig. 15a and 15b show pulse height spectra of 0.511 MeV γ-rays from a ^{22}Na source for LYSO plates after 9.5×10^{13}p/cm^2 by 67 MeV protons and 7.4×10^{13}p/cm^2 by 24 GeV protons respectively. No light output loss was observed.

Fig.16a-d compare the transmittance spectra measured for LYSO plates of $14 \times 14 \times 1.5$ mm before and after 24 GeV proton irradiation. The samples 583, 594, 609 and 001 were irradiated to 7.4×10^{13}, 2.3×10^{15}, 2.3×10^{15} and 6.9×10^{15}p/cm^2 respectively. No damage was observed in the sample 583, which is consistent with the observation shown in Fig. 15. Consistent damage was observed for two plates 594 and 609 with the values of EWLT and the RIAC at 430 nm of 74.6% and 34 m^{-1} respectively after 2.3×10^{15}p/cm^2. The values of EWLT and the RIAC at 430 nm are 72.6% and

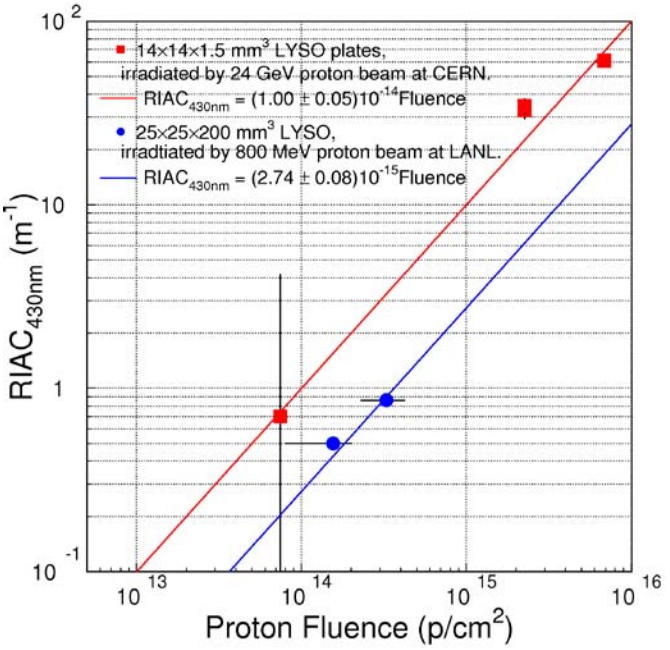

Fig. 17. The RIAC values at 430 nm are shown as a function of the proton fluence for long LYSO sample and thin plates of $14 \times 14 \times 1.5$ mm^3 after 800 MeV and 24 GeV proton irradiation respectively.

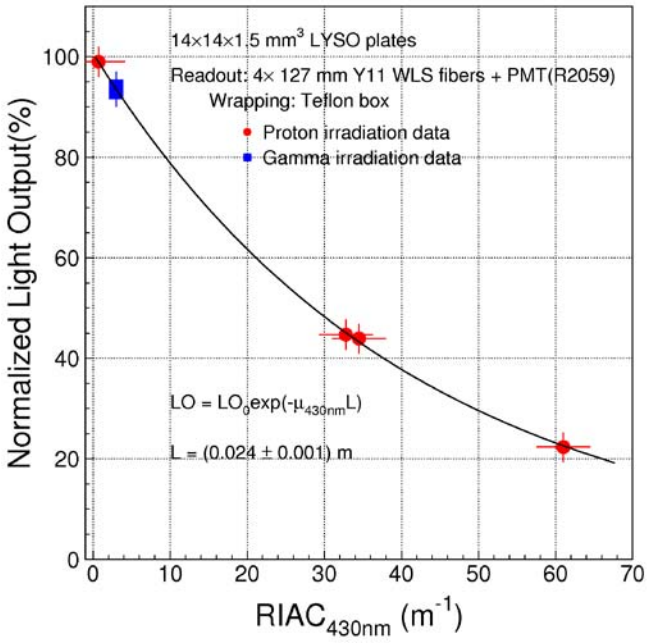

Fig. 18. The light output loss is shown as a function of RIAC@430 nm for LYSO plates of $14 \times 14 \times 1.5$ mm^3

61 m^{-1} respectively for the samples 001 after 6.9×10^{15} p/cm^2. Since the charged hadron fluence is expected to be 3×10^{14} /cm^2 at the highest rapidity for the CMS endcap calorimeter at the HL-LHC, this result shows clearly that the thin LYSO plates will survive well the HL-LHC.

Fig. 17 shows the RIAC values at 430 nm as a function of the proton fluence for the 20 cm long LYSO sample irradiated by 800 MeV protons to 1.6×10^{14} and 3.3×10^{14} p/cm^2 at LANSCE and the four $14 \times 14 \times 1.5$ mm^3 LYSO plates irradiated by 24 GeV protons at CERN from 7.4×10^{13} to 6.9×10^{15} p/cm^2. Both data groups can be described by linear fits. A factor of three difference is found between these two sets of data, which is attributed to multiple Coulomb scattering and hadronic shower leakage of 800 MeV protons in the first nuclear interaction length of 20 cm in LYSO.

Fig.18 shows the normalized light output loss as a function of the RIAC values at 430 nm for $14 \times 14 \times 1.5$ mm^3 LYSO plates. The light output of these plates was measured by four Y-11 wavelength shifting fibers coupled to a PMT as shown in Fig. 6. The RIAC value at 430 nm of 3 m^{-1} after 3×10^{14} p/cm^2 irradiation causes a light output loss of about 6% for $14 \times 14 \times 1.5$ mm^3 plates with WLS readout. The exponential fit for the light output versus the RIAC values at 430 nm indicates an average of 2.4 cm path length of the LYSO scintillation light in the $14 \times 14 \times 1.5$ mm^3 plates. It is interesting to note that the light output losses caused by protons and γ-rays are consistent: about 6% for a RIAC value at 430 nm of 3 m^{-1} which indicates a similar nature in radiation damage induced by gamma-ray dose and proton fluence. A detailed comparison between the radiation damage caused by ionization dose and charged hadrons will be discussed in our future publications.

VI. Summary and Discussion

A 15 cm long CeF_3 crystal and a 20 cm long LYSO crystal were irradiated by 800 MeV protons at LANSCE up to 3×10^{14} p/cm^2 with the crystal's longitudinal transmittance measured *in situ*. The radiation induced absorption coefficient is 17.4 m^{-1} after a proton fluence of 1.4×10^{14} p/cm^2 in the CeF_3 crystal, indicating a poor radiation hardness of this sample against protons.

The radiation induced absorption coefficient at 430 nm 0 is about 1.1 m^{-1} in the 20 cm long LYSO crystal after 3.3×10^{14} p/cm^2, which is more than one order of magnitude smaller than that in CeF_3. Similar to damages caused by ionization dose, proton-induced radiation damage in LYSO crystal shows very small to no recovery under room temperature, while that in CeF_3 recovers under room temperature [20].

Several LYSO plates of $14 \times 14 \times 1.5$ mm^3 were irradiated by 67 MeV protons at UC Davis up to 9.5×10^{13} p/cm^2 and 24 GeV protons at CERN up to 6.9×10^{15} p/cm^2. No damage was observed in LYSO plates up to 10^{14} p/cm^2 by protons of either 67 MeV or 24 GeV. The difference between the radiation induced absorption of 1.1 m^{-1} observed in the 20 cm long LYSO crystal sample after 3.3×10^{14} p/cm^2 and 3 m^{-1} observed or $14 \times 14 \times 1.5$ mm^3 LYSO plates irradiated by 24 GeV protons is due to the multiple Coulomb scattering and hadronic shower leakage. About 6% light output loss is expected for LYSO crystal plates at the highest rapidity in the CMS endcap calorimeter, indicating excellent stability of an LYSO crystal based Shashlik calorimeter at the HL–LHC.

The results of these experiments provide important information for understanding proton-induced radiation damage in fast crystal scintillators and their use in future HEP experiments at the energy and intensity frontiers. While radiation damage

induced by ionization dose is well understood [20], investigations are still on-going to understand radiation damage caused by hadrons, including both charged hadrons and neutrons. Two additional fundamental processes may cause defects by hadrons: displacement damage and nuclear breakup. While charged hadrons can produce all three types of damage (and it's often difficult to separate them), neutrons can produce only the last two, and electrons and photons produce only ionization damage. Previous studies on neutron-specific damage in lead tungstate (PWO) crystal up to 4×10^{19} n/cm^2 [21] show no neutron-specific damage [22]. Additional investigation, however, is needed to separate contributions from all three damage mechanisms in crystal scintillators.

ACKNOWLEDGMENT

This work has benefited from the use of proton beams in the LANSCE facility at LANL, the Crocker facility at UC Davis and the IRRAD facility at CERN. The authors would like to thank Dr. R. Hirosky and Dr. M. Mulhearn, who helped to irradiate the LYSO plates at UC Davis, and F. Ravotti and D. Bailleux, who helped us to irradiate the LYSO plates at CERN. Many useful discussions with Dr. G. Dissertori, Dr. F. Nessi-Tedaldi and Dr. C. Woody are acknowledged.

REFERENCES

[1] S. Chatrchyan *et al.*, "Observation of a new boson at a mass of 125 GeV with the CMS experiment at the LHC," *Phys. Lett. B*, vol. 716, pp. 30–61, Sep. 2012.

[2] R.-Y. Zhu, "Precision lead tungstate crystal calorimeter for CMS at LHC," *IEEE Trans. Nucl. Sci.*, vol. 51, no. 4, pp. 1560–1567, Aug. 2004.

[3] C. Biino, "The CMS electromagnetic calorimeter: Overview, lessons learned during run 1 and future projections," *J. Phys., Conf. Ser.*, vol. 587, no. 1, p. 012001, 2015.

[4] B. Bilki, "CMS forward calorimeters phase II upgrade," *J. Phys., Conf. Ser.*, vol. 587, no. 1, p. 012014, 2015.

[5] L. Y. Zhang, R. H. Mao, F. Yang, and R.-Y. Zhu, "LSO/LYSO crystals for calorimeters in future HEP experiments," in *Proc. IEEE Nucl. Sci. Symp. Med. Imag. Conf. (NSS/MIC)*, vol. 61. Oct. 2014, pp. 1–6.

[6] R. Becker *et al.*, "Proof-of-principle of a new geometry for sampling calorimetry using inorganic scintillator plates," *J. Phys., Conf. Ser.*, vol. 587, no. 1, p. 012039, 2015.

[7] G. Pezzullo *et al.*, "The LYSO crystal calorimeter for the Mu2e experiment," *J. Instrum.*, vol. 9, p. C03018, Mar. 2014.

[8] *Super B Conceptual Design Report*, document INFN/AE-07/2, SLAC-R-856, LAL 07-15, Mar. 2007.

[9] *The COMET Conceptual Design Report*, document J_PARC P21, The COMET Collaboration, 2009.

[10] V. Dormenev, M. Korjik, T. Kuske, V. Mechinski, and R. W. Novotny, "Comparison of radiation damage effects in PWO crystals under 150 MeV and 24 GeV high fluence proton irradiation," *IEEE Trans. Nucl. Sci.*, vol. 61, no. 1, pp. 501–506, Feb. 2014.

[11] G. Dissertori *et al.*, "Results on damage induced by high-energy protons in LYSO calorimeter crystals," *Nucl. Instrum. Methods Phys. Res. A, Accel. Spectrom. Detect. Assoc. Equip.*, vol. 745, pp. 1–6, May 2014.

[12] E. Auffray *et al.*, "Radiation damage of LSO crystals under γ- and 24 GeV protons irradiation," *Nucl. Instrum. Methods Phys. Res. A, Accel. Spectrom. Detect. Assoc. Equip.*, vol. 721, pp. 76–82, Sep. 2013.

[13] E. Auffray, M. Korjik, and A. Singovski, "Experimental study of lead tungstate scintillator proton-induced damage and recovery," *IEEE Trans. Nucl. Sci.*, vol. 59, no. 5, pp. 2219–2223, Oct. 2012.

[14] G. Dissertori *et al.*, "A study of high-energy proton induced damage in cerium fluoride in comparison with measurements in lead tungstate calorimeter crystals," *Nucl. Instrum. Methods Phys. Res. A, Accel. Spectrom. Detect. Assoc. Equip.*, vol. 622, pp. 41–48, Oct. 2010.

[15] P. Lecomte, D. Luckey, F. Nessi-Tedaldi, F. Pauss, and D. Renker, "Comparison between high-energy proton and charged pion induced damage in PbWO4 calorimeter crystals," *Nucl. Instrum. Methods Phys. Res. A, Accel. Spectrom. Detect. Assoc. Equip.*, vol. 587, pp. 266–271, Mar. 2008.

[16] P. Lecomte, D. Luckey, F. Nessi-Tedaldi, and F. Pauss, "High-energy proton induced damage study of scintillation light output from PbWO4 calorimeter crystals," *Nucl. Instrum. Methods Phys. Res. A, Accel. Spectrom. Detect. Assoc. Equip.*, vol. 564, pp. 164–168, Aug. 2006.

[17] M. Huhtinen, P. Lecomte, D. Luckey, F. Nessi-Tedaldi, and F. Pauss, "High-energy proton induced damage in PbWO4 calorimeter crystals," *Nucl. Instrum. Methods Phys. Res. A, Accel. Spectrom. Detect. Assoc. Equip.*, vol. 545, pp. 63–87, Jun. 2005.

[18] *The ECAL Technical Design Report*, document CERN/LHCC 97-33, The CMS ECAL Collaboration, 1997.

[19] J. Chen, L. Zhang, and R.-Y. Zhu, "Large size LSO and LYSO crystal scintillators for future high-energy physics and nuclear physics experiments," *Nucl. Instrum. Methods Phys. Res. A, Accel. Spectrom. Detect. Assoc. Equip.*, vol. 572, pp. 218–224, Mar. 2007.

[20] F. Yang, L. Zhang, and R.-Y. Zhu, "Gamma-ray induced radiation damage up to 340 Mrad in various scintillation crystals," *IEEE Trans. Nucl. Sci.*, vol. 63, no. 2, pp. 612–619, Apr. 2016.

[21] R. Chipaux, M. V. Korzhik, A. Borisevich, P. Lecoq, and C. Dujardin, in *Proc. 8th Int. Conf. Inorganic Scintillators (SCINT)*, 2005, p. 369.

[22] P. Adzic *et al.*, "Performance and operation of the CMS electromagnetic calorimeter," *J. Instrum.*, vol. 5, no. 3, p. 03010, 2010.